Pictorial Essay | Neuroimaging and Head & Neck

eISSN 2005-8330
https://doi.org/10.3348/kjr.2022.0101
Korean J Radiol 2022;23(6):649-663

Korean Journal of Radiology
KJR

Magnetic Resonance Imaging in Diplopia: Neural Pathway, Imaging, and Clinical Correlation

Jae Hyoung Kim, Minjae Kim, Yun Jung Bae

All authors: Department of Radiology, Seoul National University College of Medicine, Seoul National University Bundang Hospital, Seongnam, Korea

The role of magnetic resonance imaging (MRI) in diplopia is to diagnose various diseases that occur along the neural pathway governing eye movement. However, the lesions are frequently small and subtle and are therefore difficult to detect on MRI. This article presents representative cases of diseases that cause diplopia. The purpose of this article was to 1) describe the anatomy of the neural pathway governing eye movement, 2) recommend optimal MRI targets and protocols for the diagnosis of diseases causing diplopia, 3) correlate MRI findings with misalignment of the eyes (i.e., strabismus), and 4) help familiarize the reader with the imaging diagnosis of diplopia.

Keywords: *MRI; Diplopia; Neural pathway*

INTRODUCTION

Strabismus and Diplopia

Diplopia is one of the major reasons for performing brain magnetic resonance imaging (MRI). Pathologies affecting the neural pathway that governs eye movement cause misalignment of the eyes (i.e., strabismus), and consequently, binocular diplopia. Congenital strabismus is not frequently associated with diplopia because subconscious adaptation to avoid diplopia occurs in the brain by suppression of the image from one eye [1]. However, acquired strabismus is inevitably accompanied by diplopia. In many cases, however, strabismus is very subtle and difficult to recognize despite diplopia.

Neural Pathway of Eye Movement

The neural pathway governing eye movement is complex and difficult to explain briefly. It begins in the cerebral cortex or other brain regions, including the cerebellum and vestibular nuclei [2]. Two cortical areas that are well known for providing signals for eye movement are the frontal eye field and parieto-occipito-temporal cortex. They are connected to the gaze centers in the brainstem and, finally to the 3rd, 4th, and 6th cranial nerves. The extraocular muscles in the orbit are innervated by the cranial nerves. The 4th cranial nerve innervates the superior oblique muscle, which moves the eyeball inferomedially. The 6th cranial nerve innervates the lateral rectus muscle and abducts the eyeball. The 3rd cranial nerve innervates other extraocular muscles (superior, inferior, medial rectus, and inferior oblique muscles) (Fig. 1).

Symptoms differ depending on the location of the lesion along the neural pathway from the cerebral cortex to the eyeball. Lesions in the cerebral cortex cause eyeball deviation but not diplopia [2]. Lesions in the brainstem involving the gaze centers or cranial nerve nuclei, along the course of the cranial nerves (i.e., in the cistern, cavernous sinus, and orbit), or in the extraocular muscles cause binocular diplopia. Lesions in the eyeball can cause monocular diplopia.

Many diseases affect the neural pathways governing eye movement, which can result in binocular diplopia [3-5]. Instead of describing the MRI findings of individual disease entities, the purpose of this article is to propose

Received: February 18, 2022 **Revised:** March 14, 2022
Accepted: March 18, 2022
Corresponding author: Jae Hyoung Kim, MD, PhD, Department of Radiology, Seoul National University College of Medicine, Seoul National University Bundang Hospital, 82 Gumi-ro 173beon-gil, Bundang-gu, Seongnam 13620, Korea.
• E-mail: jaehkim@snu.ac.kr

MRI targets in the neural pathway and recommend optimal MRI protocols for the identification of diplopia (Table 1). We also correlated the MRI findings with strabismus to help the reader become familiar with the imaging diagnosis of diplopia.

MRI of the Brainstem

MRI Targets

The gaze centers; the 3rd, 4th, and 6th nerve nuclei; and their connecting fibers are the targets of MRI. The neural pathway governing eye movement is located longitudinally at the dorsal aspect of the brainstem just anterior to the

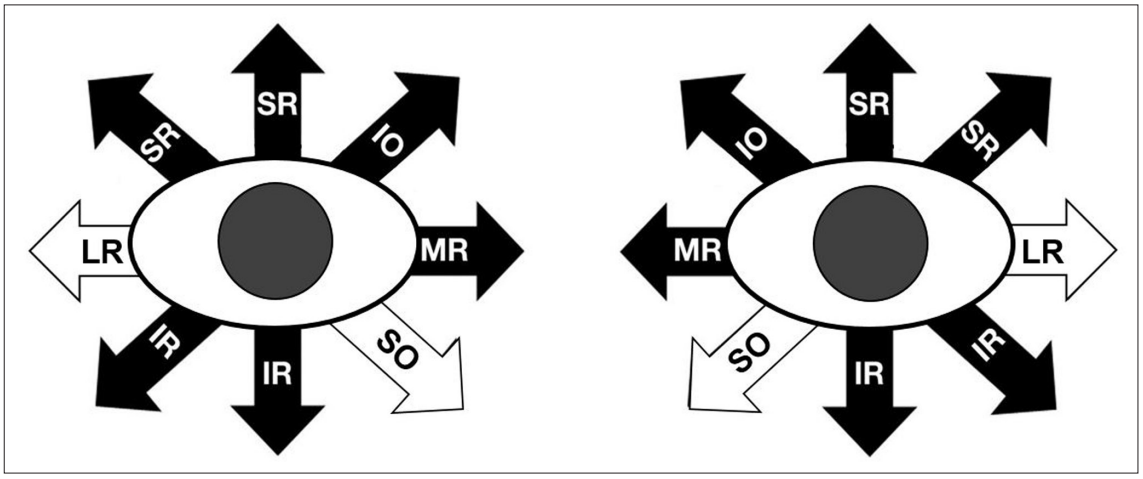

Fig. 1. Schematic drawing of the actions of the extraocular muscles. Arrows indicate the direction of eye movement due to contraction of each muscle. IO = inferior oblique, IR = inferior rectus, LR = lateral rectus, MR = medial rectus, SO = superior oblique, SR = superior rectus

Table 1. MRI Targets in Neural Pathway, MRI Protocols and Diseases Causing Diplopia

MRI Targets in Neural Pathway	MRI Protocols	Diseases
Brainstem		
3rd nerve nucleus	Routine brain protocol	Stroke
4th nerve nucleus	Thin-section DWI	Demyelinating disease
6th nerve nucleus		Inflammation
Medial longitudinal fasciculus		Tumors
		Others
Cistern		
3rd nerve	High-resolution T2 imaging	Congenital agenesis or hypoplasia of 3rd,
4th nerve	Thin-section postcontrast T1 imaging	4th or 6th nerves
6th nerve	Orbital thin-section coronal T1 or T2 imaging*	Inflammation
		Trauma
		Tumors
		Aneurysm
		Fistula
		Others
Cavernous sinus		
3rd nerve	High-resolution fat-suppressed postcontrast T1	Microvascular cranial nerve palsy
4th nerve	imaging	Inflammation
6th nerve		Fistula
		Aneurysm
		Tumors
		Others

*Orbital coronal imaging is needed to evaluate the size of the extraocular muscles, particularly in pediatric paralytic strabismus and chronic diplopia in adults. DWI = diffusion-weighted imaging

https://doi.org/10.3348/kjr.2022.0101

Korean Journal of Radiology
KJR

aqueduct and 4th ventricle in the midbrain and pons (Fig. 2) [2]. There are two gaze centers: the vertical gaze center in the midbrain and the horizontal gaze center in the pons.

The paramedian pontine reticular formation (PPRF), the horizontal gaze center, is located close to the 6th nerve nucleus. For horizontal conjugate eye movement, the PPRF sends a signal to the ipsilateral 6th nerve nucleus, which then projects two types of signals (Fig. 2). One signal is transmitted to the ipsilateral lateral rectus muscle and the other to the contralateral 3rd nerve nucleus, via a fiber tract known as the medial longitudinal fasciculus (MLF) to contract the contralateral medial rectus muscle [6].

MRI Protocol

Any disease focally involving the aforementioned neural pathway in the brainstem (such as acute stroke, tumor, demyelinating disease, or inflammatory disease) causes isolated diplopia. Therefore, a routine brain MRI protocol is needed with additional MRI sequences when indicated. Small acute infarction is one of the causative diseases of sudden onset isolated diplopia in elderly individuals. Therefore, thin-section diffusion-weighted imaging (DWI) with a slice thickness of 2–3 mm is recommended.

Cases

Three types of ocular motor palsy affect horizontal conjugate movement: lateral gaze palsy, internuclear ophthalmoplegia, and one-and-a-half syndrome [2,7,8].

Lateral gaze palsy indicates paresis of abduction in the ipsilateral eye and conjugate paresis of adduction in the contralateral eye. It is caused by a lesion involving the PPRF or the 6th nerve nucleus (Fig. 3). Peripheral 6th nerve palsy is distinct from lateral gaze palsy, where the lesion involves only the peripheral 6th cranial nerve, not the 6th nerve nucleus (Fig. 4). Therefore, only abduction of the ipsilateral eye is paralyzed.

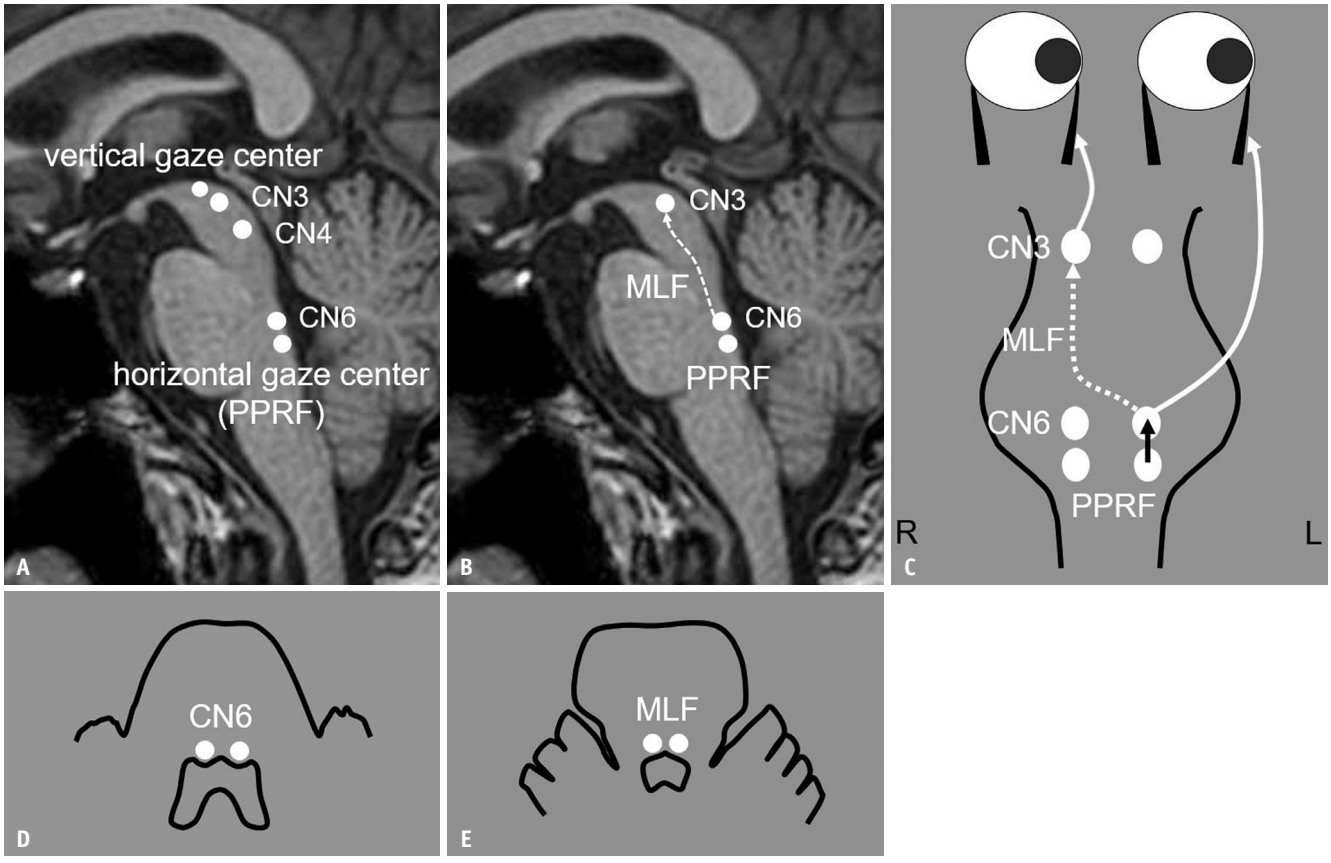

Fig. 2. Neural pathway for eye movement in the brainstem.
A. Sagittal T1-weighted image shows the neural pathway including the vertical gaze center, CN3, CN4, CN6, and horizontal gaze center (PPRF), which are located longitudinally from superior to inferior. **B, C.** Sagittal T1-weighted image **(B)** and coronal diagram **(C)** show the pathway for leftward horizontal eye movement, where the left PPRF sends signals to CN6 and CN3 through the MLF. **D.** In the axial diagram, white circles indicate the location of CN6 at the facial colliculus of the lower pons. PPRF is known to lie inferiorly to CN6. **E.** In the axial diagram, white circles indicate the MLF located along the posterior margin of the mid and upper pons. CN3 = 3rd nerve nucleus, CN4 = 4th nerve nucleus, CN6 = 6th nerve nucleus, MLF = medial longitudinal fasciculus, PPRF = paramedian pontine reticular formation

https://doi.org/10.3348/kjr.2022.0101

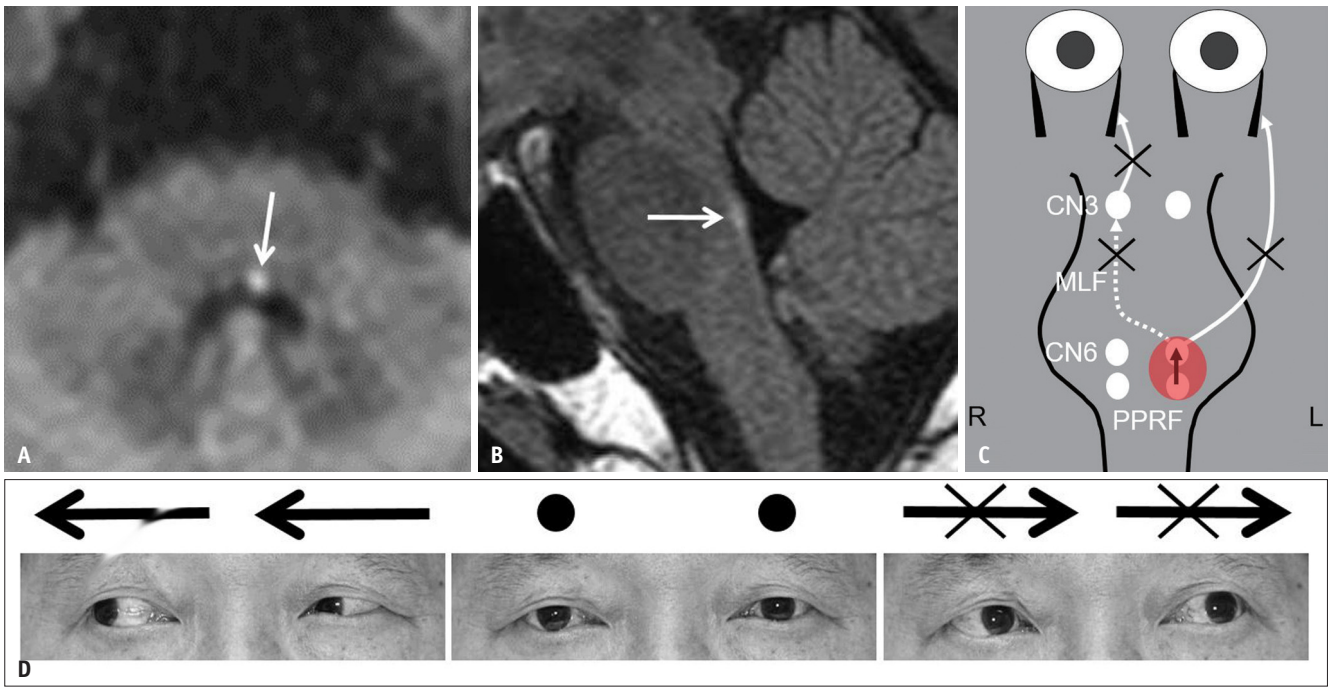

Fig. 3. Lateral gaze palsy in a 44-year-old male with acute infarction.
A, B. Axial diffusion-weighted image **(A)** and sagittal fluid-attenuated inversion recovery image **(B)** showing a small acute infarction in the left pontine facial colliculus area (arrows), which corresponds to the location of the CN6. **C.** Diagram shows the mechanism of lateral gaze palsy: an infarction (red circle) involving the left PPRF or left CN6. **D.** Gaze photographs show impaired abduction of the left eye and impaired adduction of the right eye with a leftward gaze. With a rightward gaze, both eye movements are normal. CN3 = 3rd nerve nucleus, CN6 = 6th nerve nucleus, MLF = medial longitudinal fasciculus, PPRF = paramedian pontine reticular formation, X = interruption of signal transmission or eye movement

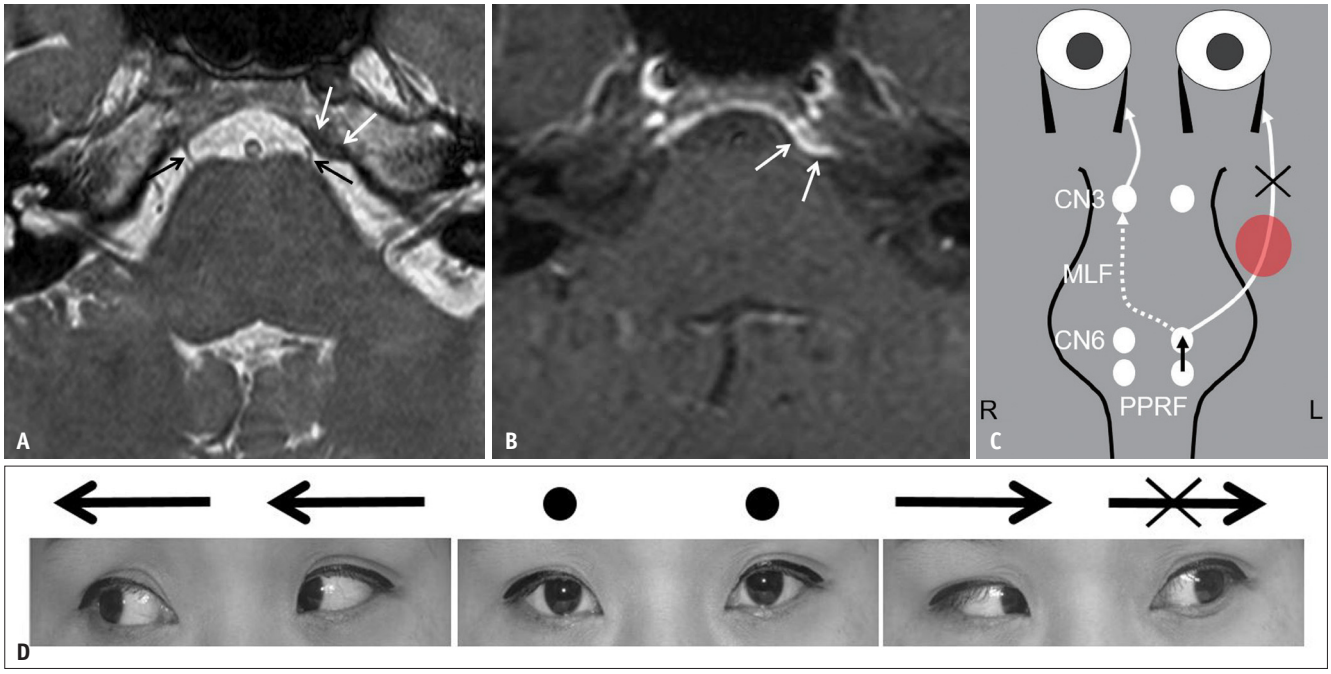

Fig. 4. Peripheral 6th nerve palsy in a 52-year-old female with meningioma.
A, B. Axial high-resolution T2 image **(A)** and axial post-contrast T1 image **(B)** showing a small meningioma in the left petroclival area (white arrows). The left 6th nerve (black arrow) is compressed by the tumor. Normal right 6th nerve (black arrow). **C.** Diagram shows the mechanism of peripheral 6th nerve palsy: an infarction (red circle) involving the left peripheral 6th nerve. **D.** Gaze photographs show impaired abduction of only the left eye with leftward gaze. CN3 = 3rd nerve nucleus, CN6 = 6th nerve nucleus, MLF = medial longitudinal fasciculus, PPRF = paramedian pontine reticular formation, X = interruption of signal transmission or eye movement

https://doi.org/10.3348/kjr.2022.0101

Korean Journal of Radiology
KJR

Internuclear ophthalmoplegia implies paresis of adduction in the ipsilateral eye, but normal conjugate abduction of the contralateral eye. Internuclear ophthalmoplegia occurs with lesions involving the MLF (Fig. 5).

One-and-a-half syndrome is characterized by a combination of lateral gaze palsy in one direction and internuclear ophthalmoplegia in the other and is induced by a lesion involving the 6th nerve nucleus and the adjacent MLF (Fig. 6).

In addition to these types of conjugate palsy, lesions involving only the 3rd or 4th nerve nucleus cause nonconjugate paresis of the affected eye (Fig. 7) [8].

MRI in the Cistern

MRI Targets

The 3rd, 4th and 6th cranial nerves traversing the cistern towards the cavernous sinus are the targets of MRI. The 3rd nerve nuclei are located in the upper midbrain ventrolateral to the aqueduct at the level of the superior colliculus [2]. The nerves traverse the midbrain towards the lower interpeduncular cistern, where they exit the brainstem and run through the cistern towards the cavernous sinus (Fig. 8).

The 4th nerve nuclei are located ventrolateral to the aqueduct in the lower midbrain at the level of the inferior colliculus [2]. The nerves travel dorsally and decussate before exiting the brainstem at the level of the inferior margin of the inferior colliculus. They then run in the anterolateral direction through the ambient cistern towards the cavernous sinus (Fig. 9).

The 6th nerve nuclei are located in the facial colliculus of the lower pons [2]. The nerves run across the lower pons towards the ponto-medullary sulcus, where they exit the brainstem and travel in the superior direction through the prepontine cistern towards Dorello's canal (Fig. 10).

MRI Protocol

For imaging of the cranial nerves in the cistern, high-resolution T2 MRI sequencing is recommended because it can depict the morphology of the cranial nerves with high contrast to the cerebrospinal fluid (Figs. 8-10). Therefore, high-resolution T2 imaging is essential for pediatric strabismus with the possibility of congenital agenesis or hypoplasia of the 3rd, 4th, and 6th cranial nerves [9-

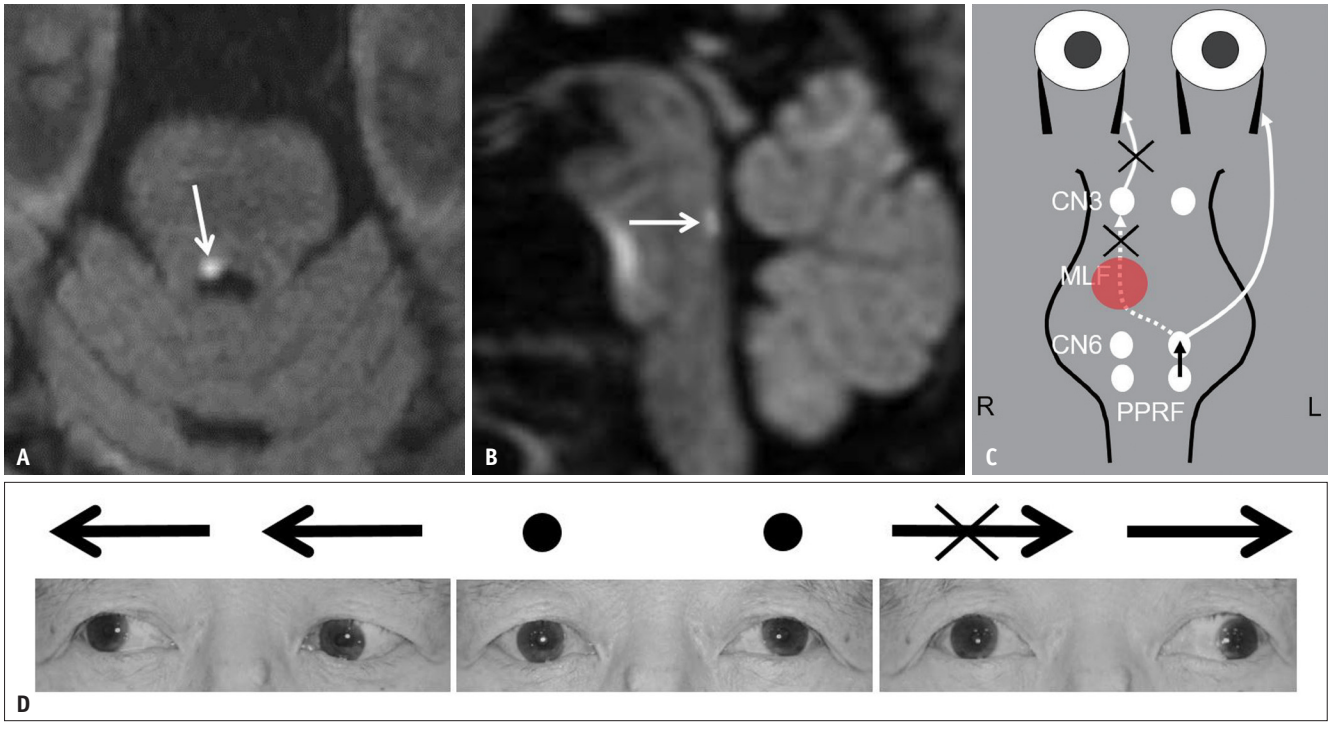

Fig. 5. Internuclear ophthalmoplegia in a 62-year-old male with acute infarction.
A, B. Axial **(A)** and sagittal **(B)** diffusion-weighted images show a small acute infarction in the posterior pons (arrows), where the right MLF is located. **C.** Diagram shows the mechanism for internuclear ophthalmoplegia, with an infarction (red circle) involving the right MLF. **D.** Gaze photographs show impaired adduction of the right eye with leftward gaze. All other eye movements are also preserved. CN3 = 3rd nerve nucleus, CN6 = 6th nerve nucleus, MLF = medial longitudinal fasciculus, PPRF = paramedian pontine reticular formation, X = interruption of signal transmission or eye movement

https://doi.org/10.3348/kjr.2022.0101

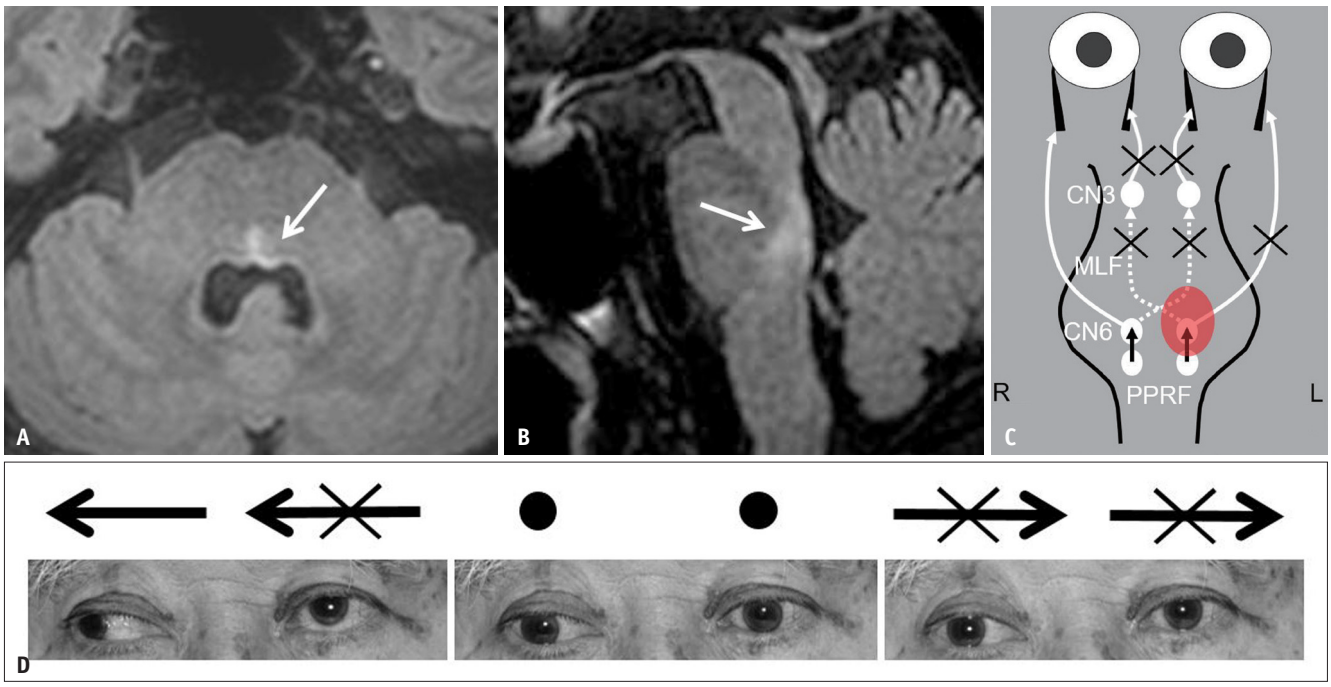

Fig. 6. One-and-a-half syndrome in a 73-year-old male with multiple sclerosis.
A, B. Axial **(A)** and sagittal **(B)** fluid-attenuated inversion recovery images showing a small plaque in the left pontine facial colliculus area (arrows). The plaque may involve the left CN6 and the adjacent left MLF. **C.** Diagram shows the mechanism for one-and-a-half syndrome: the plaque (red circle) involves both the left CN6 (or the PPRF) and left MLF. **D.** Gaze photographs show impaired movement of both eyes with leftward gaze (i.e., lateral gaze palsy), and impaired adduction of the left eye with rightward gaze (i.e., internuclear ophthalmoplegia). Only abduction of the right eye was normal. CN3 = 3rd nerve nucleus, CN6 = 6th nerve nucleus, MLF = medial longitudinal fasciculus, PPRF = paramedian pontine reticular formation, X = interruption of signal transmission or eye movement

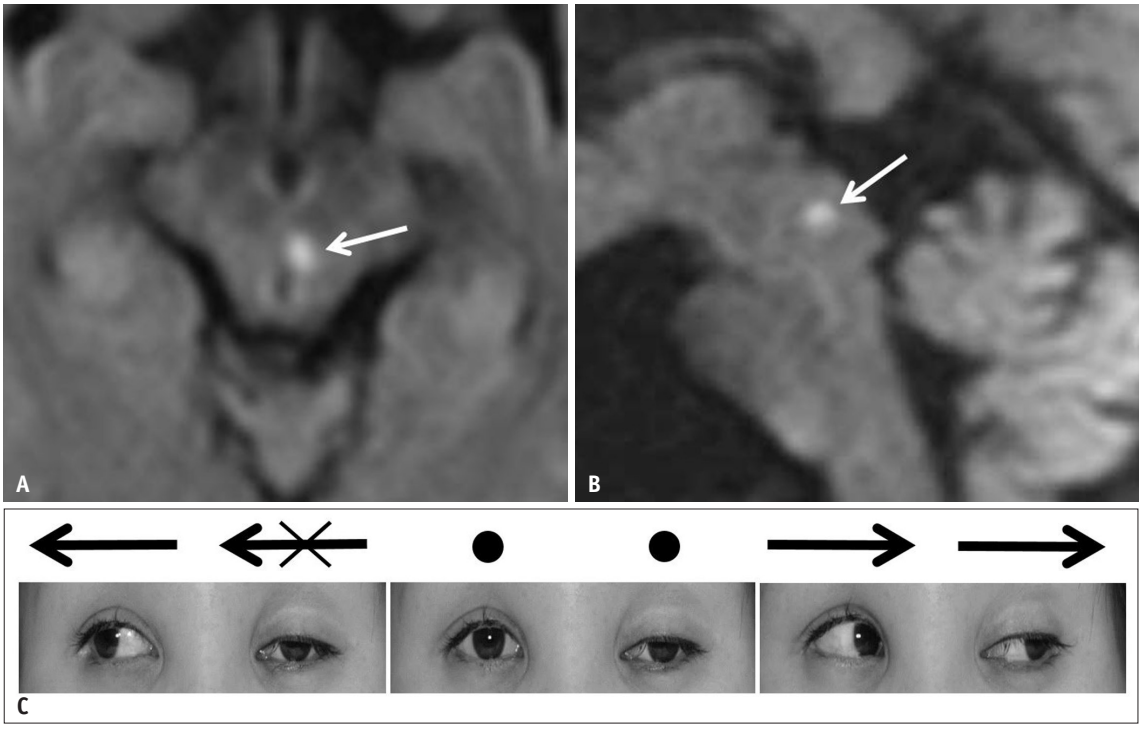

Fig. 7. Third nerve palsy in a 40-year-old female with both horizontal and vertical diplopia.
A, B. Axial **(A)** and sagittal **(B)** diffusion-weighted images showing a small acute infarction in the upper midbrain ventrolateral to the aqueduct (arrows), which corresponds to the location of the left 3rd nerve nucleus. **C.** Gaze photographs show ptosis and impaired adduction of the left eye. The supraduction and infraduction of the left eye were also impaired (not shown). X = interruption of eye movement

https://doi.org/10.3348/kjr.2022.0101

Korean Journal of Radiology
KJR

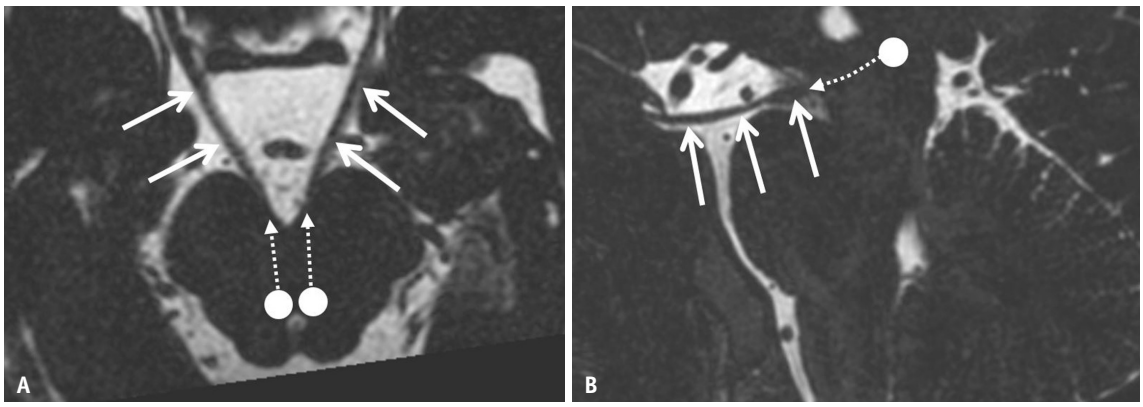

Fig. 8. Third nerve in the cistern.
A, B. Reformatted axial **(A)** and sagittal **(B)** high-resolution T2 images show the path of the 3rd nerve in the midbrain (dotted arrows) and cistern (arrows). White circles indicate bilateral 3rd nerve nuclei.

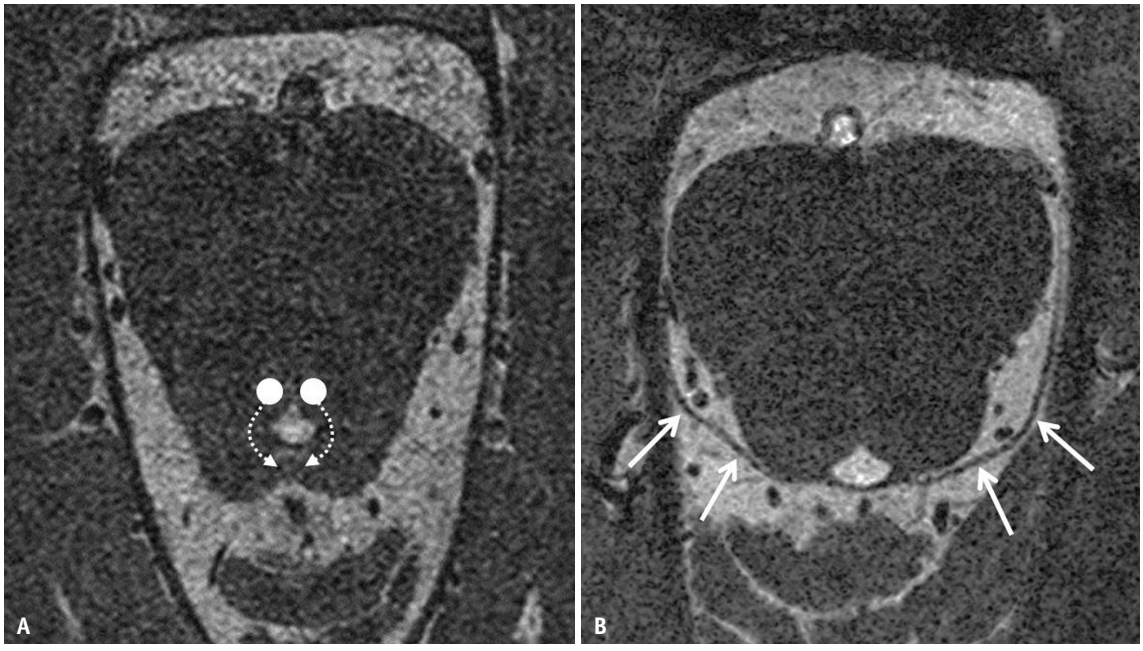

Fig. 9. Fourth nerve in the cistern.
A. Axial super-high-resolution T2 image obtained at the level of the inferior colliculus shows the path of the 4th nerve in the midbrain (dotted arrows). **B.** Another image at the level of the inferior margin of the inferior colliculus shows the 4th nerve in the cistern (arrows). White circles indicate bilateral 4th nerve nuclei.

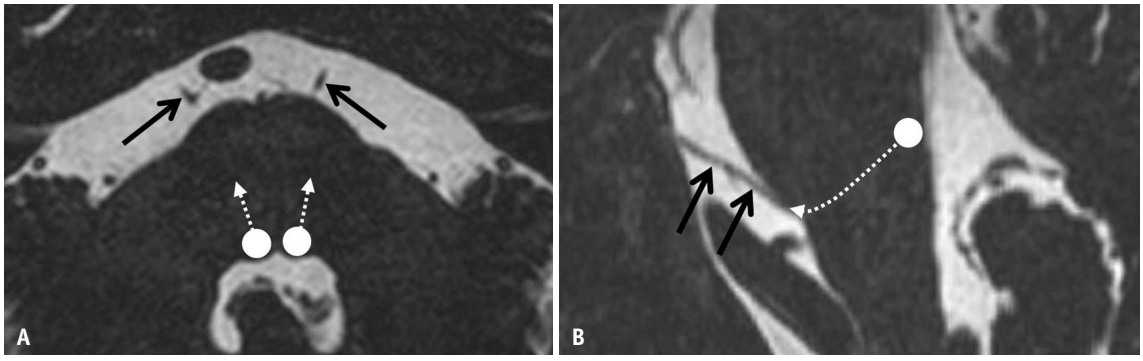

Fig. 10. Sixth nerve in the cistern.
A, B. Axial **(A)** and reformatted sagittal **(B)** high-resolution T2 images show the path of the 6th nerve in the pons (dotted arrows) and cistern (arrows). White circles indicate the bilateral 6th nerve nuclei.

https://doi.org/10.3348/kjr.2022.0101

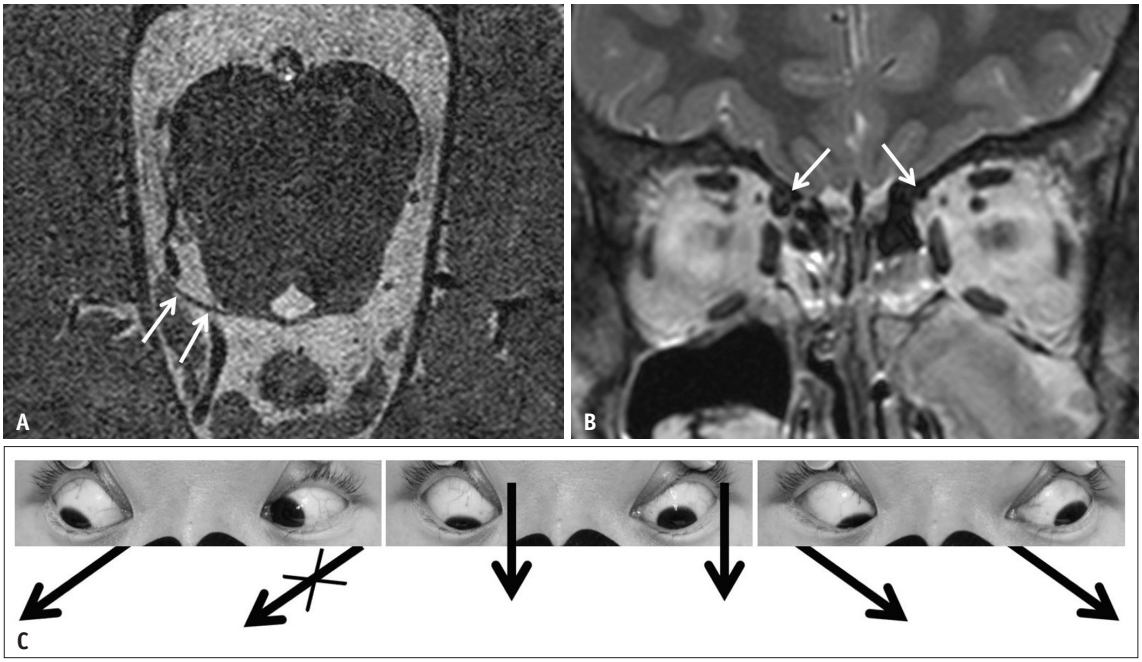

Fig. 11. Congenital agenesis of the 4th nerve in a 15-year-old boy.
A. Axial high-resolution T2 image shows the normal right 4th nerve (arrows). The left 4th nerve could not be identified. **B.** The orbital coronal T2 image shows atrophy of the left superior oblique (arrows). **C.** Gaze photographs show impaired movement of the left eye in the medial-inferior direction. X = interruption of eye movement

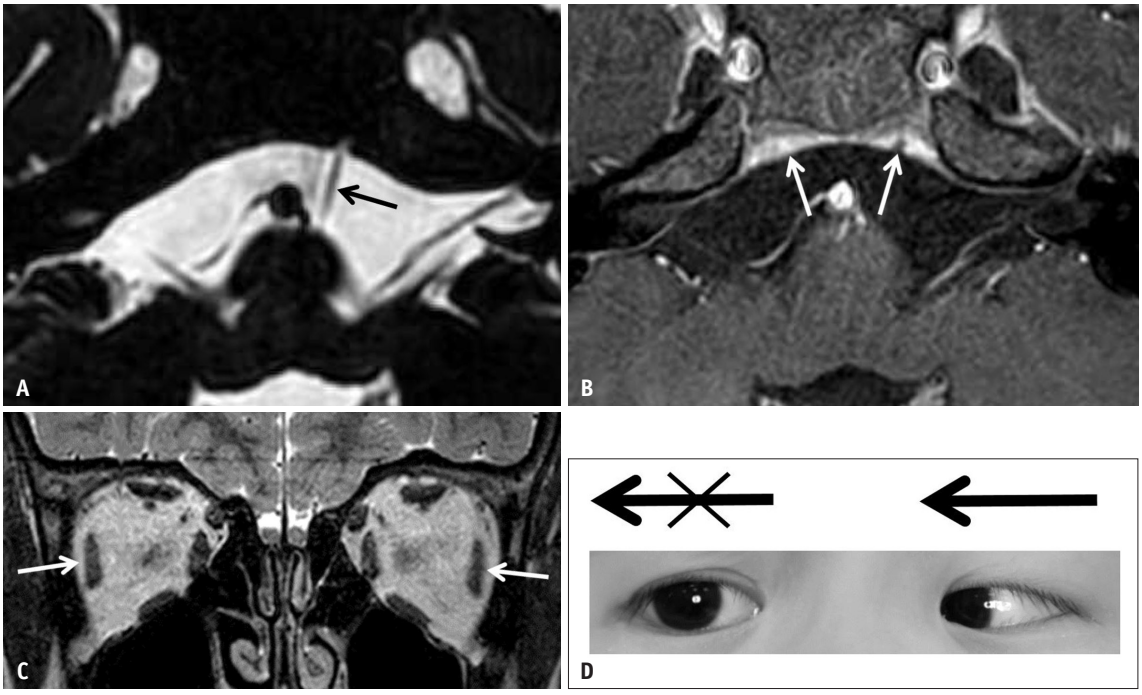

Fig. 12. Congenital agenesis of the 6th nerve (Duane's retraction syndrome, type I) in a 5-year-old boy.
A. Axial high-resolution T2 image showing a normal left 6th nerve (arrow). The right 6th nerve was not observed. **B.** Axial thin-section post-contrast T1 image shows atresia of the right Dorello's canal (arrow), compared with the normal left side (arrow). **C.** Orbital coronal T2 image shows symmetrical size of the bilateral lateral recti (arrows). The volume of the lateral rectus is preserved because of aberrant innervation from the 3rd nerve in this disease. **D.** This is different from acquired 6th nerve palsy. Gaze photograph showing impaired abduction of the right eye. X = interruption of eye movement

https://doi.org/10.3348/kjr.2022.0101

Korean Journal of Radiology
KJR

11]. In addition, as T2 imaging enables delineation of the course of the cisternal segment of the cranial nerves, it can be used to detect lesions causing extrinsic compression of the cranial nerves, such as aneurysms or tumors. Both fast gradient echo and spin echo techniques can be used for this purpose. The fast gradient-echo based techniques include constructive interference in steady state (CISS), balanced turbo field echo (bTFE), and fast imaging employing steady state acquisition (FIESTA); and the fast spin-echo based techniques include driven equilibrium radiofrequency reset pulse (DRIVE), T2 volumetric isotropic turbo spin-echo acquisition (VISTA), fast recovery fast spin-echo (FRFSE), and T2 sampling perfection with application-optimized contrasts by using different flip angle evolutions (SPACE) [12-14].

Concerning the spatial resolution of high-resolution T2 imaging, the voxel size of 0.6 x 0.6 x 0.6 mm is sufficient for evaluation of the 3rd and 6th cranial nerves [11,15]. However, super-high-resolution imaging is needed to evaluate the 4th cranial nerve, which is the smallest (0.5–1.1 mm in diameter) among all cranial nerves [16]. A previous article [17] reported that MRI with a voxel size of 0.3 x 0.3 x 0.25 mm at 3 tesla identified the 4th cranial nerves in 100% of 32 normal subjects.

Thin-section post-contrast T1 imaging with a slice thickness ≤ 2 mm is also recommended for the diagnosis of various acquired diseases in which contrast enhancement of the affected nerves or adjacent structures may be observed [12,14,18]. Additionally, orbital thin-section coronal T1 or T2 imaging with a slice thickness ≤ 2 mm is needed to evaluate the size of the extraocular muscles, particularly in pediatric paralytic strabismus and chronic diplopia in adults.

Cases

Congenital agenesis or hypoplasia of the 3rd, 4th and 6th cranial nerves should be considered in pediatric strabismus. They account for approximately 5% of all pediatric strabismus cases, according to unpublished hospital data. Agenesis of the 4th cranial nerve was the most common (> 90%) (Fig. 11) and agenesis of the 6th cranial nerve was the second most common (≤ 10%) (Fig. 12). Hypoplasia or agenesis of the 3rd cranial nerve is rare (Fig. 13).

Diseases such as microvascular cranial nerve palsy,

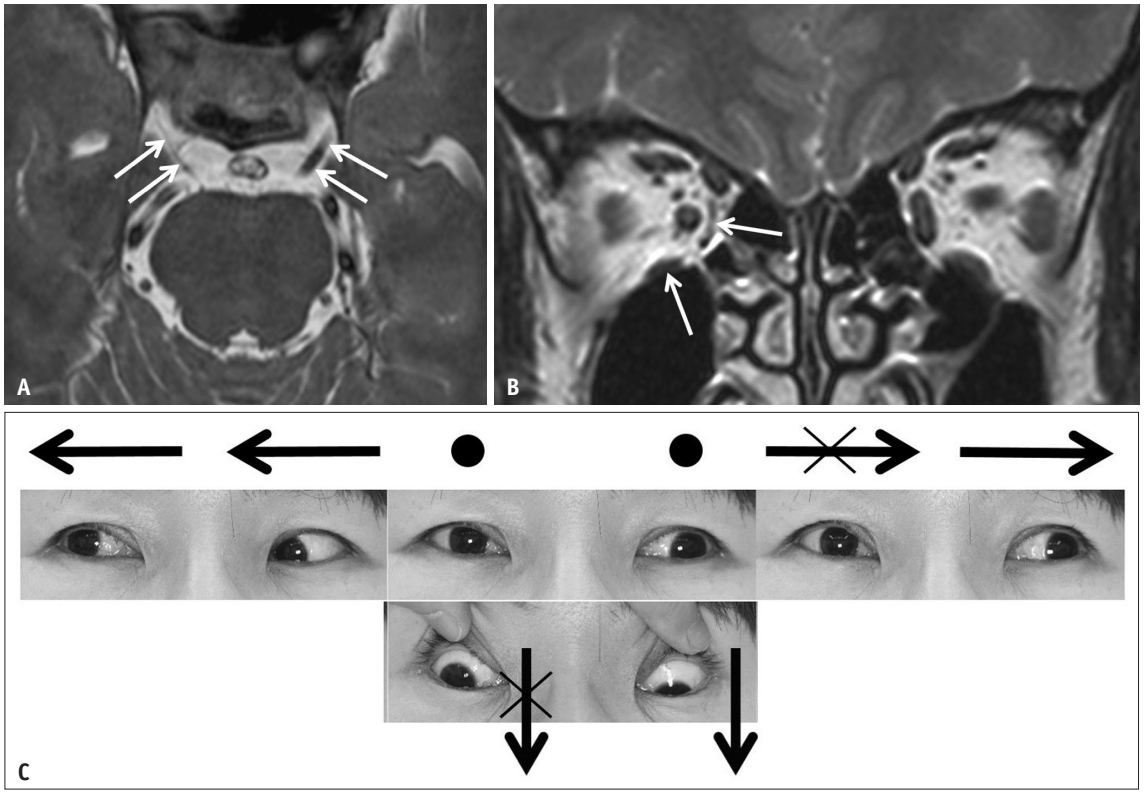

Fig. 13. Congenital hypoplasia of the 3rd nerve in a 40-year-old female.
A. Axial high-resolution T2 image shows the hypoplastic right 3rd nerve (arrows) compared with the normal left 3rd nerve (arrows). **B.** Orbital coronal T2 image shows atrophy of the right medial and inferior recti (arrows). **C.** Gaze photographs show impaired adduction and infraduction of the right eye. X = interruption of eye movement

https://doi.org/10.3348/kjr.2022.0101

inflammatory disease, trauma, tumors, aneurysm, and fistula may be responsible for acquired isolated diplopia [3,4,19]. Among these, inflammatory disease (Fig. 14), trauma (Figs. 15, 16), tumors (Fig. 4), and aneurysms may involve the cisternal segment of the cranial nerves [20-24].

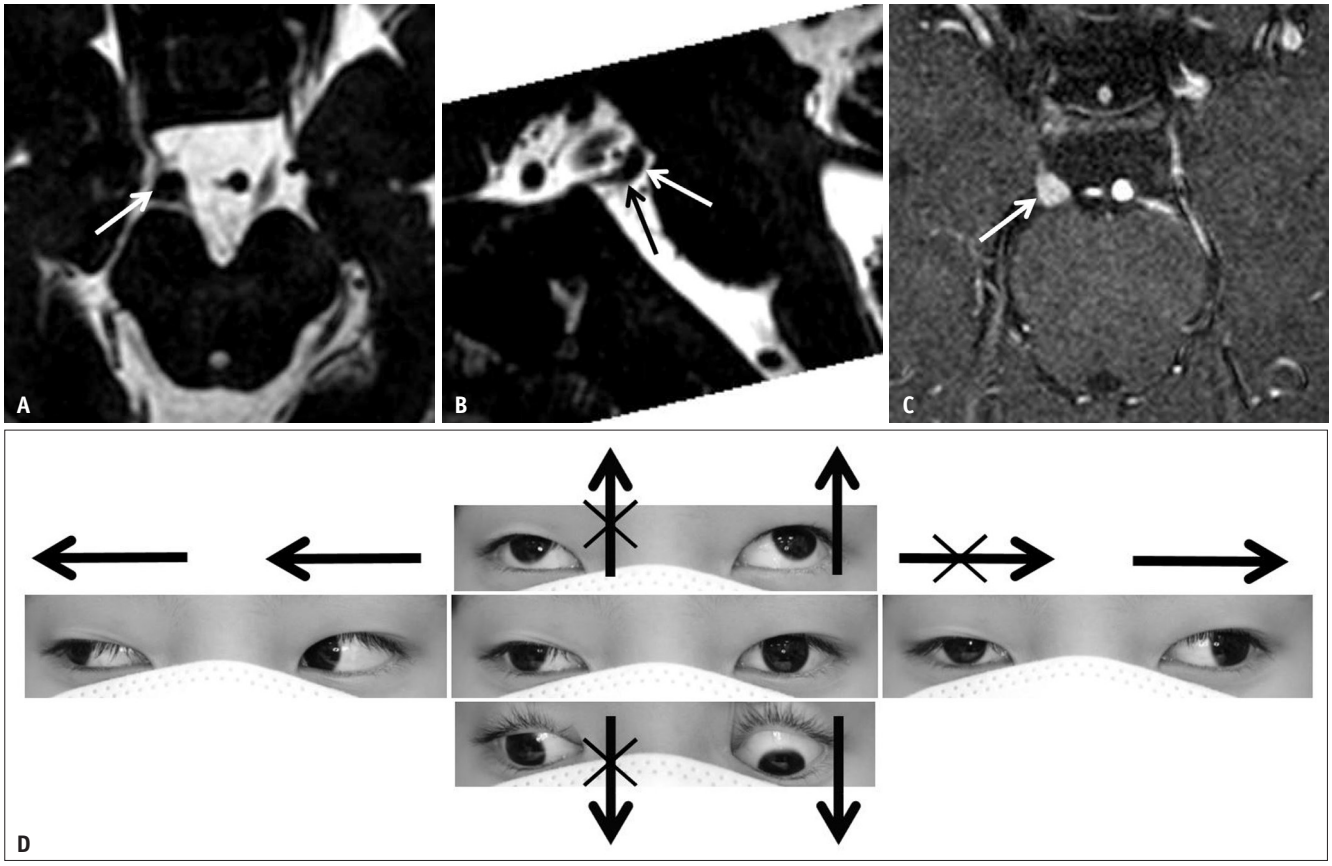

Fig. 14. Ophthalmoplegic migraine in an 8-year-old male.
A-C. Axial **(A)** and reformatted sagittal **(B)** high-resolution T2 images and axial thin-section postcontrast T1 image **(C)** show focal thickening and enhancement of the right 3rd nerve at the proximal cisternal segment (arrows). **D.** Gaze photographs show ptosis and impaired adduction, supraduction, and infraduction of the right eye. X = interruption of eye movement

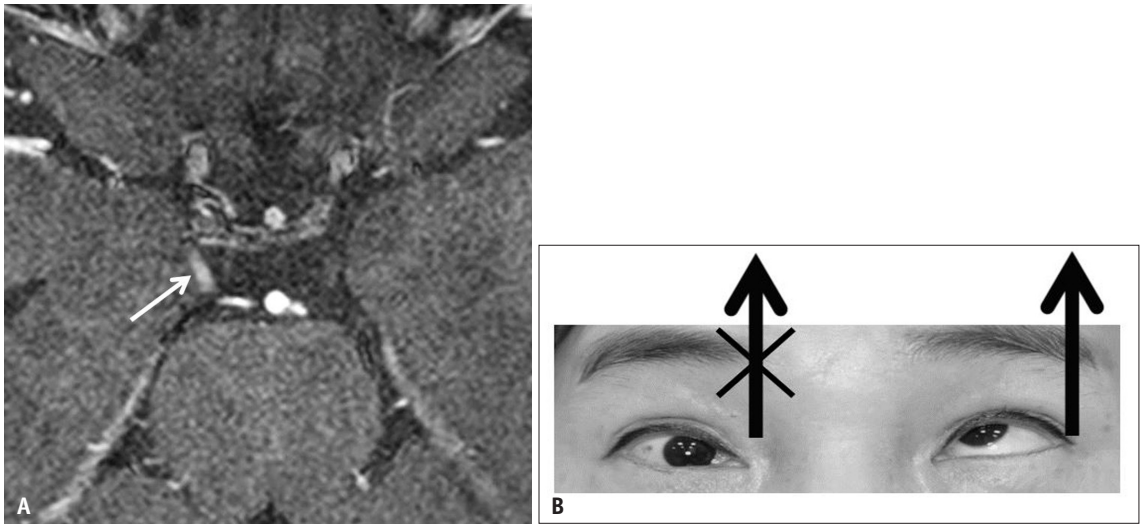

Fig. 15. Recent traumatic injury of the 3rd nerve in a 49-year-old female.
A. Axial thin-section post-contrast T1 image shows enhancement of the right 3rd nerve at the cisternal segment (arrow). **B.** Gaze photograph shows ptosis and impaired supraduction of the right eye. X = interruption of eye movement

https://doi.org/10.3348/kjr.2022.0101

Korean Journal of Radiology
KJR

MRI of the Cavernous Sinus

MRI Targets

The 3rd, 4th, and 6th cranial nerves passing through the cavernous sinus are the targets of MRI. The 3rd cranial nerve, 4th cranial nerve, ophthalmic division, and maxillary division of the 5th cranial nerve run in the lateral wall of the cavernous sinus in that order from superior to inferior (Fig. 17). The 6th cranial nerve lies more medially towards the internal carotid artery [25].

MRI Protocol

For imaging of the cranial nerves in the cavernous sinus, high-resolution postcontrast T1 imaging with a slice thickness ≤ 1 mm is recommended [5,12,26]. This sequence allows the course of the cranial nerves in the cavernous

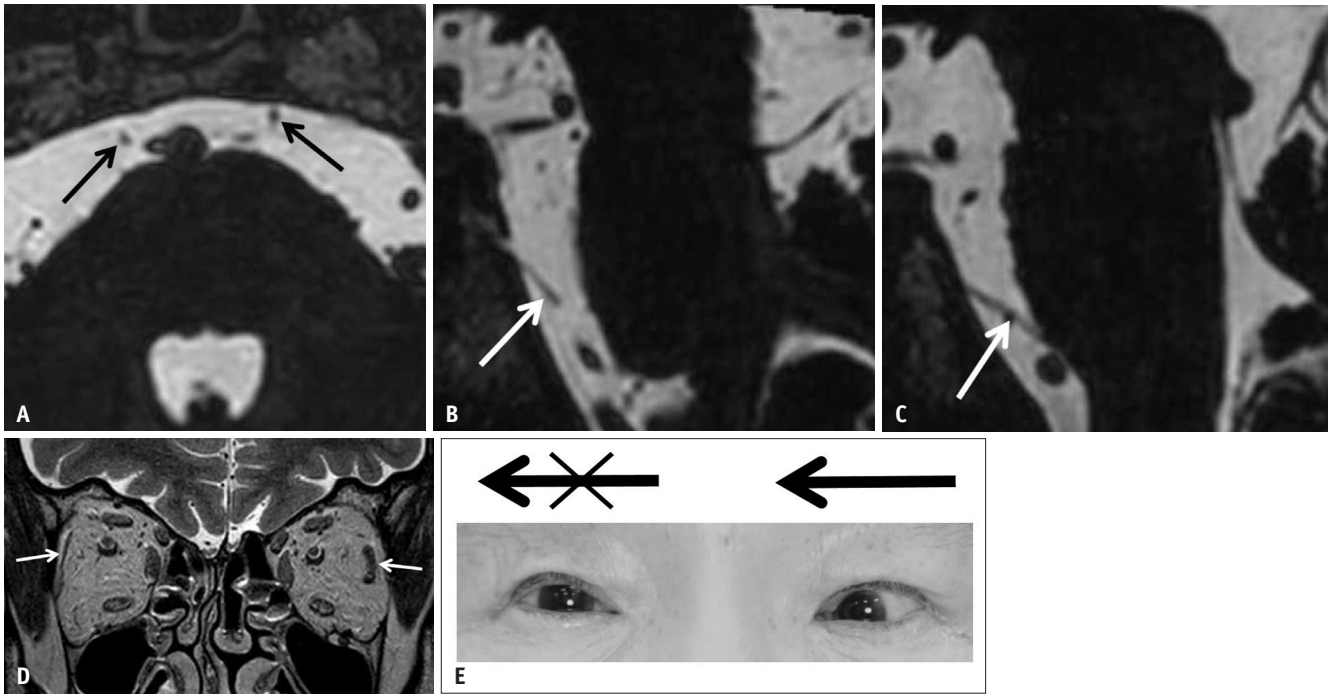

Fig. 16. Chronic traumatic injury of the 6th nerve in a 78-year-old female.
A. Axial high-resolution T2 image shows normal-appearing 6th nerve bilaterally at the upper cisternal segment (arrows). **B, C.** Reformatted sagittal high-resolution T2 images show amputation of the right 6th nerve (arrow in **B**) compared to the normal left 6th nerve (arrow in **C**). **D.** Orbital coronal T2 image shows chronic atrophy of the right lateral rectus (arrows). **E.** Gaze photograph shows impaired abduction of the right eye. X = interruption of eye movement

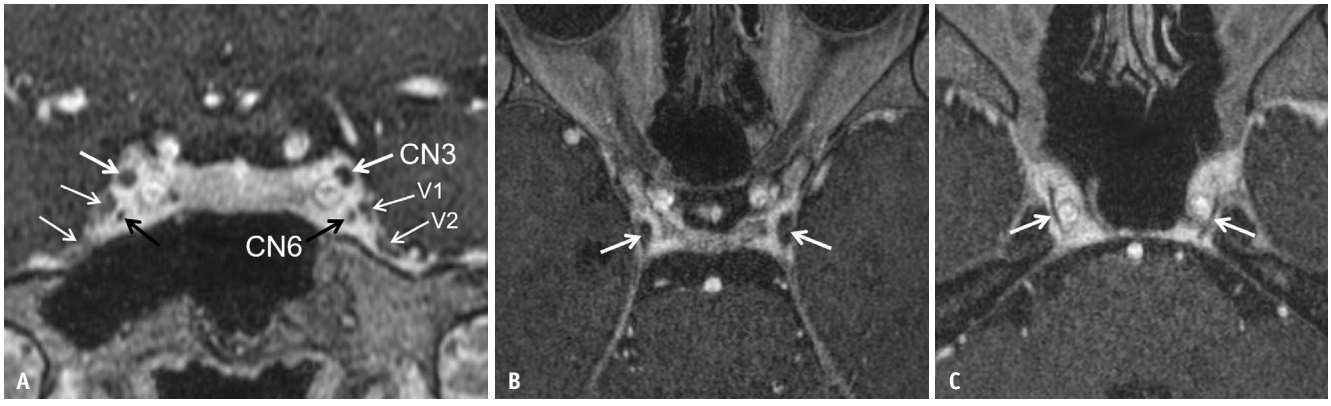

Fig. 17. Cranial nerves in the cavernous sinus.
A. Coronal high-resolution post-contrast T1 image shows the path of the cranial nerves in the cavernous sinus as non-enhancing dark signals (arrows). **B, C.** Axial high-resolution post-contrast T1 images show the path of the 3rd nerve (arrows in **B**) and 6th nerve (arrows in **C**) in the cavernous sinus. CN3 = 3rd nerve, CN6 = 6th nerve, V1 = the ophthalmic division of the 5th cranial nerve, V2 = maxillary division of the 5th cranial nerve

https://doi.org/10.3348/kjr.2022.0101

sinus to be identified as non-enhancing dark signals with good contrast to the enhancing cavernous sinus (Fig. 17). The 3rd cranial nerve is almost always located in the upper lateral portion of the cavernous sinus, the 4th cranial nerve is barely visible because of its small size, and the 6th cranial nerve is observed at a variable rate, depending on the spatial resolution of MRI.

Employing the fat-suppression technique enables better

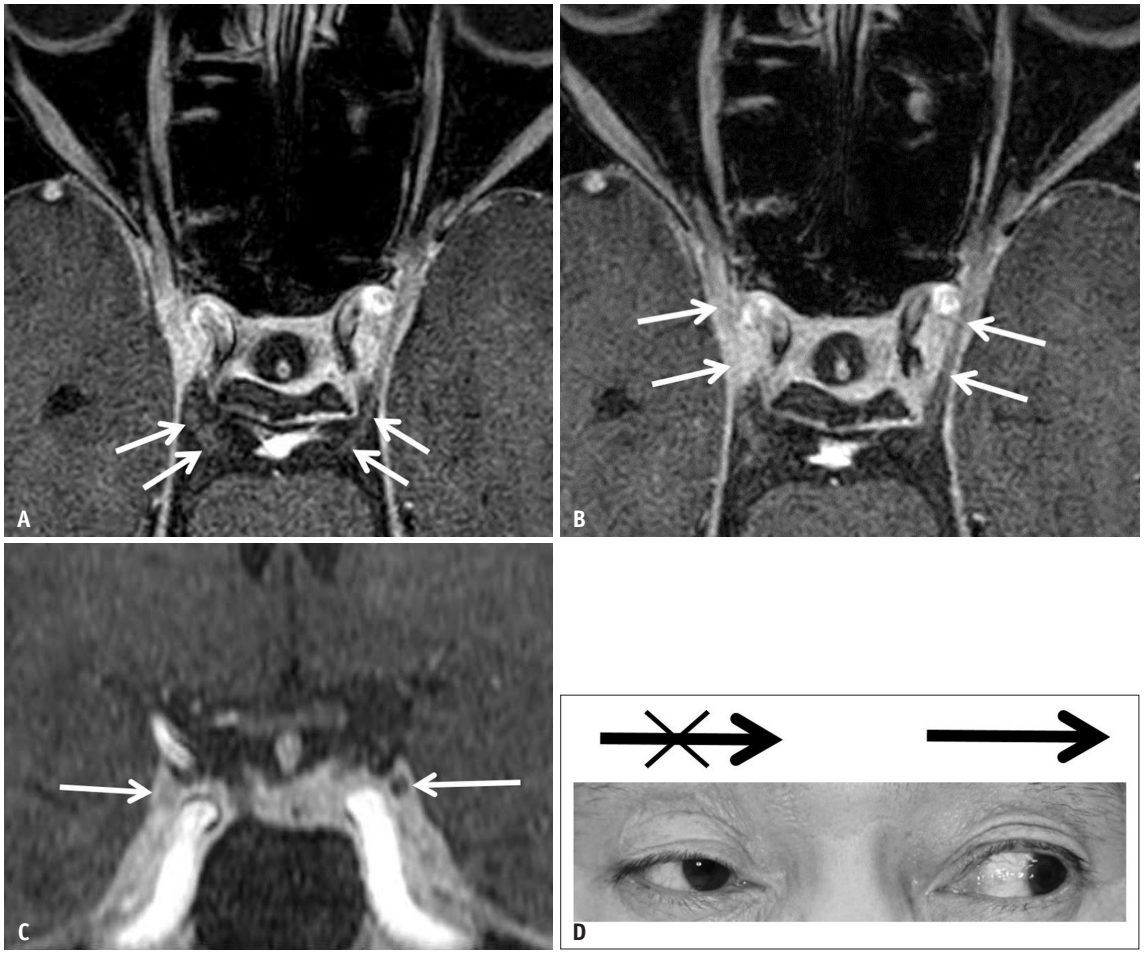

Fig. 18. Microvascular ischemia of the 3rd nerve in a 62-year-old male.
A-C. Axial **(A, B)** and coronal **(C)** high-resolution fat-suppressed post-contrast T1 images show no enhancement of the 3rd nerve at the cisternal segment (arrows in **A**), but subtle enhancement of the right 3rd nerve at the cavernous sinus segment (arrows in **B, C**). **D.** Gaze photograph shows ptosis and impaired adduction of the right eye. X = interruption of eye movement

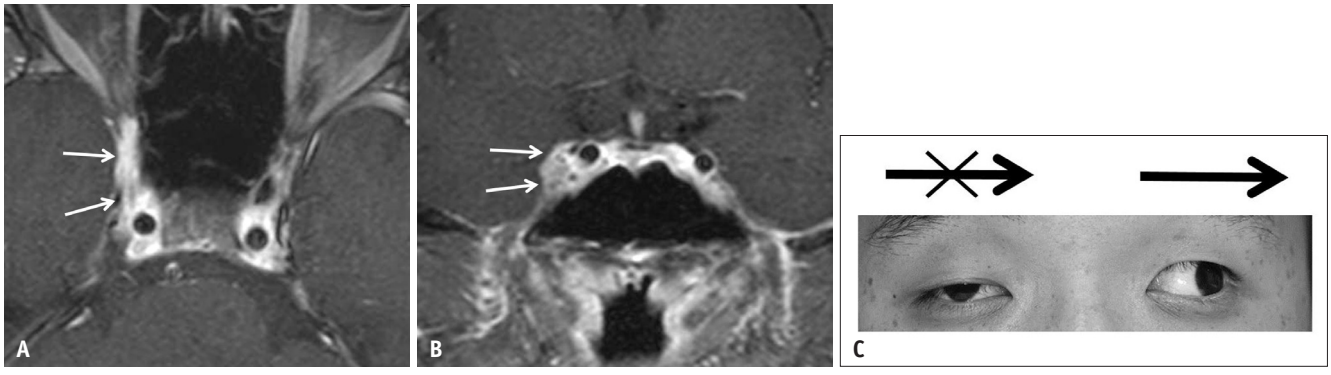

Fig. 19. Tolosa-Hunt syndrome in a 22-year-old male.
A, B. Axial thin-section fat-suppressed post-contrast T1 images show focal bulging enhancement in the right cavernous sinus extending anteriorly to the orbital apex (arrows). **C.** Gaze photograph shows ptosis and impaired adduction of the right eye. X = interruption of eye movement

https://doi.org/10.3348/kjr.2022.0101

Korean Journal of Radiology
KJR

evaluation of cranial nerve enhancement in the orbit and cavernous sinus [27]. In terms of slice thickness, in our experience, ≤ 1 mm is recommended to detect subtle enhancement of the cranial nerves. Superior lesion detection can be achieved with a higher spatial resolution.

Cases

In pediatric strabismus, no particular diseases appear to affect the cavernous sinus. In acquired isolated diplopia, diseases such as microvascular cranial nerve palsy (Fig. 18), inflammatory disease (Fig. 19), fistula (Fig. 20), aneurysm, and tumors affect the cranial nerves within the cavernous sinus [3-5,28,29].

Microvascular cranial nerve palsy is the most common cause of sudden onset isolated diplopia in elderly individuals, affecting the 3rd, 4th, or 6th cranial nerves [3,4]. It is more common in patients with vascular risk factors, such as diabetes mellitus and hypertension, and is therefore often referred to as diabetic palsy. In a recent study [27], most patients with 3rd nerve palsy due to

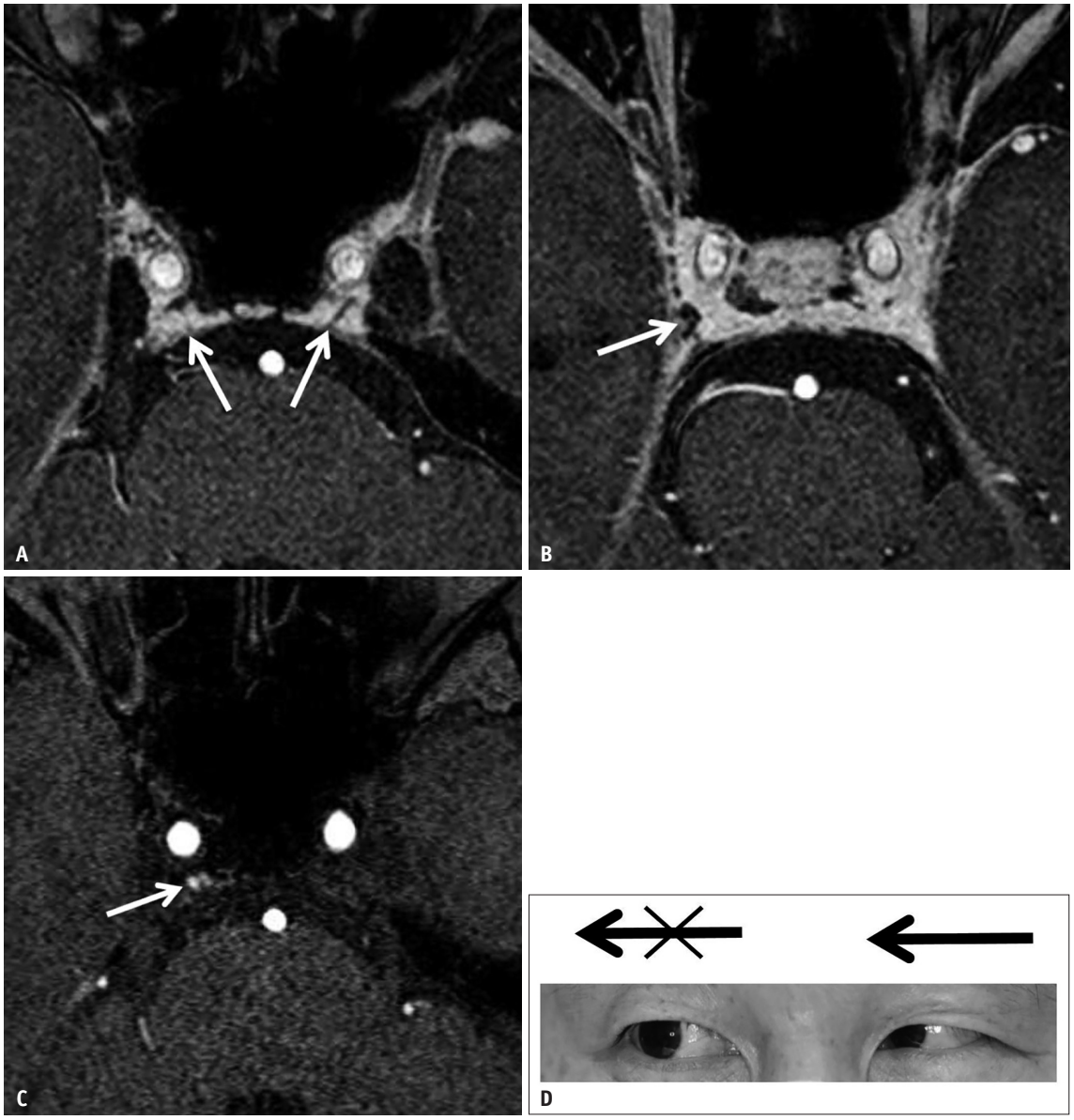

Fig. 20. Small cavernous dural arteriovenous fistula in a 49-year-old male.
A. Axial high-resolution fat-suppressed post-contrast T1 image shows obliteration of the right Dorello's canal (arrow) compared with the normal left side (arrow). **B.** A few slices up, another image shows a small signal void in the right cavernous sinus (arrow), indicating the possibility of a small fistula. **C.** MR angiography source image shows a small, high signal in the right cavernous sinus (arrow), also supporting the diagnosis of a small fistula. **D.** Gaze photograph shows impaired abduction of the right eye. X = interruption of eye movement

https://doi.org/10.3348/kjr.2022.0101

presumed microvascular ischemia showed enhancement of the 3rd cranial nerve in the cavernous sinus. In our experience, enhancement of the 3rd cranial nerve frequently extends anteriorly to the level of the orbital apex, but rarely to the cisternal segment of the nerve.

CONCLUSION

The causes of diplopia are diverse and are difficult to differentiate clinically. Therefore, MRI should cover the neural pathway governing eye movement and target the brainstem and the course of the 3rd, 4th, and 6th cranial nerves in the cistern, cavernous sinus, and orbit. The MRI protocol should include high-resolution T2 imaging and high-resolution fat-suppressed post-contrast T1 imaging to detect frequently small and subtle lesions. As an additional MRI sequence, thin-section DWI is essential to diagnose small acute infarctions in the brainstem in sudden onset diplopia in elderly individuals. Super high-resolution T2 imaging is needed to evaluate the 4th cranial nerve in pediatric paralytic strabismus.

Availability of Data and Material

All data generated or analyzed during the study are included in this published article.

Conflicts of Interest

The authors have no potential conflicts of interest to disclose.

Author Contributions

Conceptualization: Jae Hyoung Kim. Data curation: Jae Hyoung Kim. Formal analysis: Jae Hyoung Kim. Funding acquisition: Jae Hyoung Kim. Investigation: Jae Hyoung Kim. Methodology: all authors. Project administration: Jae Hyoung Kim. Resources: all authors. Software: Jae Hyoung Kim. Supervision: Jae Hyoung Kim. Validation: Jae Hyoung Kim. Visualization: Jae Hyoung Kim. Writing—original draft: Jae Hyoung Kim. Writing—review and editing: Minjae Kim.

ORCID iDs

Jae Hyoung Kim
https://orcid.org/0000-0002-0545-4138
Minjae Kim
https://orcid.org/0000-0002-5382-9360
Yun Jung Bae
https://orcid.org/0000-0002-1779-4949

Funding Statement

None

REFERENCES

1. Economides JR, Adams DL, Horton JC. Perception via the deviated eye in strabismus. *J Neurosci* 2012;32:10286-10295
2. Blumenfeld H. *Neuroanatomy through clinical cases*. Sunderland: Sinauer Associate, 2002:528-553
3. Choi KD, Choi SY, Kim JS, Choi JH, Yang TH, Oh SY, et al. Acquired ocular motor nerve palsy in neurology clinics: a prospective multicenter study. *J Clin Neurol* 2019;15:221-227
4. Tamhankar MA, Biousse V, Ying GS, Prasad S, Subramanian PS, Lee MS, et al. Isolated third, fourth, and sixth cranial nerve palsies from presumed microvascular versus other causes: a prospective study. *Ophthalmology* 2013;120:2264-2269
5. Mahalingam HV, Mani SE, Patel B, Prabhu K, Alexander M, Fatterpekar GM, et al. Imaging spectrum of cavernous sinus lesions with histopathologic correlation. *Radiographics* 2019;39:795-819
6. Miller MJ, Mark LP, Ho KC, Haughton VM. Anatomic relationship of the oculomotor nuclear complex and medial longitudinal fasciculus in the midbrain. *AJNR Am J Neuroradiol* 1997;18:111-113
7. Bronstein AM, Rudge P, Gresty MA, Du Boulay G, Morris J. Abnormalities of horizontal gaze. Clinical, oculographic and magnetic resonance imaging findings. II. Gaze palsy and internuclear ophthalmoplegia. *J Neurol Neurosurg Psychiatry* 1990;53:200-207
8. Bae YJ, Kim JH, Choi BS, Jung C, Kim E. Brainstem pathways for horizontal eye movement: pathologic correlation with MR imaging. *Radiographics* 2013;33:47-59
9. Yang HK, Kim JH, Hwang JM. Magnetic resonance imaging in 14 patients with congenital oculomotor nerve palsy. *Clin Neuroradiol* 2020;30:237-242
10. Kim JH, Hwang JM. Absence of the trochlear nerve in patients with superior oblique hypoplasia. *Ophthalmology* 2010;117:2208-2213
11. Kim JH, Hwang JM. Presence of the abducens nerve according to the type of Duane's retraction syndrome. *Ophthalmology* 2005;112:109-113
12. Casselman J, Mermuys K, Delanote J, Ghekiere J, Coenegrachts K. MRI of the cranial nerves--more than meets the eye: technical considerations and advanced anatomy. *Neuroimaging Clin N Am* 2008;18:197-231
13. Blitz AM, Choudhri AF, Chonka ZD, Ilica AT, Macedo LL, Chhabra A, et al. Anatomic considerations, nomenclature, and advanced cross-sectional imaging techniques for visualization of the cranial nerve segments by MR imaging. *Neuroimaging Clin N Am* 2014;24:1-15
14. Kim HJ, Seong M, Kim Y. Normal anatomy of cranial nerves III–XII on magnetic resonance imaging. *J Korean Soc Radiol* 2020;81:501-529

https://doi.org/10.3348/kjr.2022.0101

15. Kim JH, Hwang JM. Congenital monocular elevation deficiency. *Ophthalmology* 2009;116:580-584
16. Ettl A, Salomonowitz E. Visualization of the oculomotor cranial nerves by magnetic resonance imaging. *Strabismus* 2004:12:85-96
17. Choi BS, Kim JH, Jung C, Hwang JM. High-resolution 3D MR imaging of the trochlear nerve. *AJNR Am J Neuroradiol* 2010;31:1076-1079
18. Lee JH, Cheng KL, Choi YJ, Baek JH. High-resolution imaging of neural anatomy and pathology of the neck. *Korean J Radiol* 2017;18:180-193
19. Dhaliwal A, West AL, Trobe JD, Musch DC. Third, fourth, and sixth cranial nerve palsies following closed head injury. *J Neuroophthalmol* 2006;26:4-10
20. Mark AS, Casselman J, Brown D, Sanchez J, Kolsky M, Larsen TC 3rd, et al. Ophthalmoplegic migraine: reversible enhancement and thickening of the cisternal segment of the oculomotor nerve on contrast-enhanced MR images. *AJNR Am J Neuroradiol* 1998;19:1887-1891
21. Eisenhut F, Gerner ST, Goelitz P, Doerfler A, Seifert F. High-resolution magnetic resonance imaging in isolated, traumatic oculomotor nerve palsy: a case report. *Radiol Case Rep* 2021;16:384-388
22. Ravindran K, Lorensini B, Gaillard F, Kalus S. Bilateral traumatic abducens nerve avulsion: a case series and literature review. *J Clin Neurosci* 2017;44:30-33
23. Chan JW, Albretson J. Causes of isolated recurrent ipsilateral sixth nerve palsies in older adults: a case series and review of the literature. *Clin Ophthalmol* 2015;9:373-377
24. Sato M, Sonobe S, Iwabuchi N, Yoshida M, Tominaga T. Two cases of cerebral aneurysm presenting with oculomotor nerve palsy anatomically evaluated using constructive interference steady-state imaging. *Surg Cereb Stroke* 2021;49:287-291
25. Yasuda A, Campero A, Martins C, Rhoton AL Jr, de Oliveira E, Ribas GC. Microsurgical anatomy and approaches to the cavernous sinus. *Neurosurgery* 2005;56(1 Suppl):4-27
26. Linn J, Peters F, Lummel N, Schankin C, Rachinger W, Brueckmann H, et al. Detailed imaging of the normal anatomy and pathologic conditions of the cavernous region at 3 tesla using a contrast-enhanced MR angiography. *Neuroradiology* 2011;53:947-954
27. Yang Y, Lai C, Yan F, Wang J. Clinical significance of MRI contrast enhancement of the oculomotor nerve in ischemic isolated oculomotor nerve palsy. *J Clin Neurol* 2020;16:653-658
28. Jain R, Sawhney S, Koul RL, Chand P. Tolosa-Hunt syndrome: MRI appearances. *J Med Imaging Radiat Oncol* 2008;52:447-451
29. Kim E, Kim JH, Choi BS, Jung C, Lee DH. MRI and MR angiography findings to differentiate jugular venous reflux from cavernous dural arteriovenous fistula. *AJR Am J Roentgenol* 2014;202:839-846

 https://doi.org/10.3348/kjr.2022.0101